RACK1-mediated Suppression of Acinar-to-Ductal Reprogramming Blocks Inflammation and Carcinogenesis in Pancreas

Wei Zhang[1,2], Tingting Jiang[1,2], Huiqing Zhang[3], Fang Wei[1,2], Xiaojia Li[1,2]✉ and Keping Xie[1,2]✉

[1]Center for Pancreatic Cancer Research, The South China University of Technology School of Medicine, Guangzhou, Guangdong 510006, China

[2]The South China University of Technology Comprehensive Cancer Center, Guangzhou, Guangdong 510006, China

[3]The Third Department of Medical Oncology, Jiangxi Cancer Hospital, Nanchang, Jiangxi 330006, China

✉*Correspondence*: Dr. Keping Xie or Dr. Xiaojia Li, Center for Pancreatic Cancer Research, South China University of Technology School of Medicine, Guangzhou, Guangdong 510006; *Phone*: 020-3938-0579; *E-mail*: scutmedicine@scut.edu.cn or xiaojia0424@scut.edu.cn.

SUPPLEMENTARY FIGURES

Wei Zhang *et al.*, Figure S1

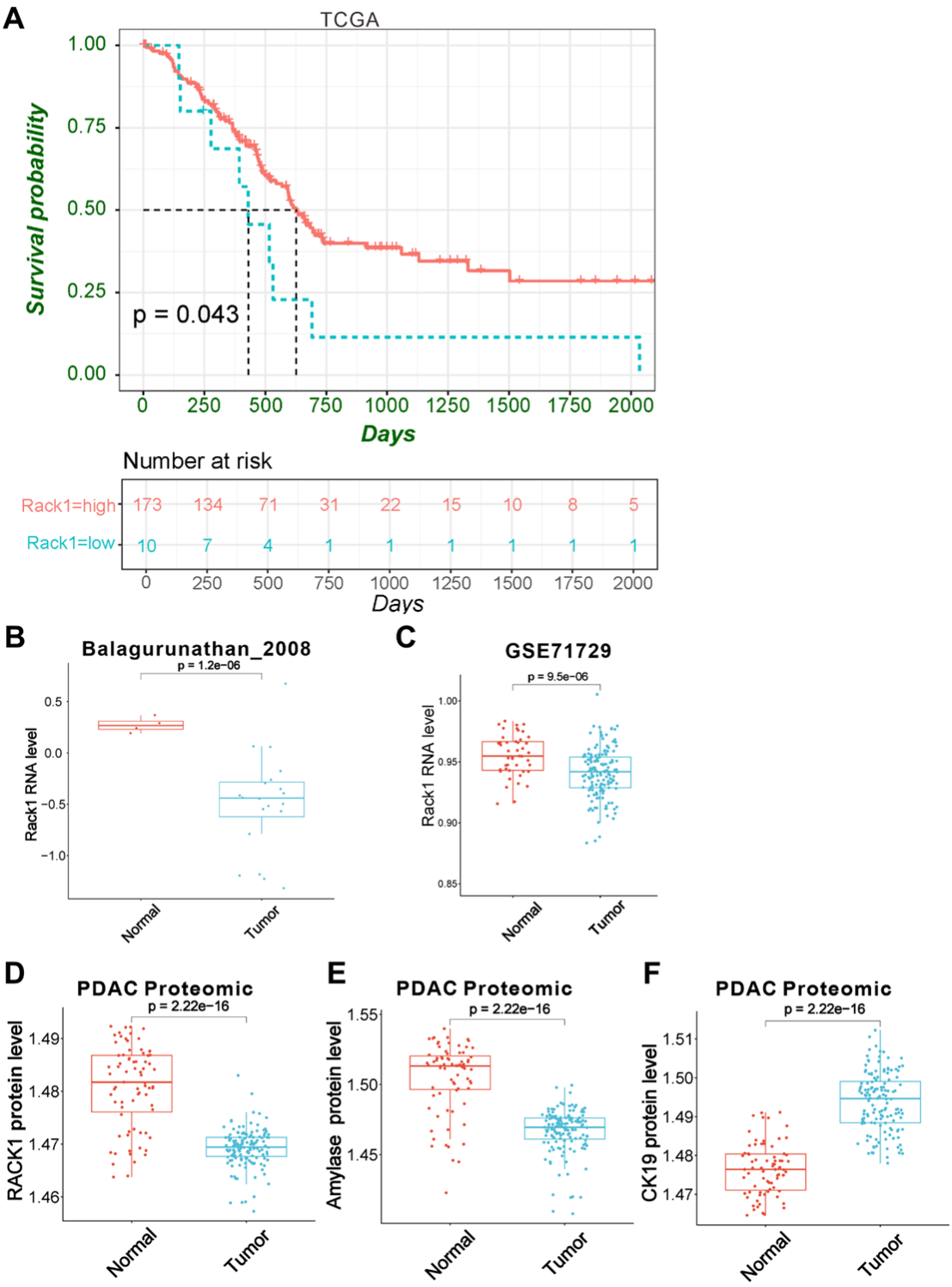

Fig. S1. RACK1 was down-regulated in PDA. (**A**) Kaplan–Meier survival curves of RACK1 protein expression in 183 PDA patients. (**B-C**) RACK1 was decreased at the mRNA level as determined by RNA-seq. (**D**) The proteomics analysis: decreased RACK1 expression in PDA tissues as compared to adjacent normal tissues. (**E**) The proteomics analysis: decreased amylase in PDA tissues as compared to adjacent normal tissues. (**F**) The proteomics analysis: up-regulated CK19 in PDA tissues as compared to adjacent normal tissues.

Wei Zhang *et al.*, Figure S2

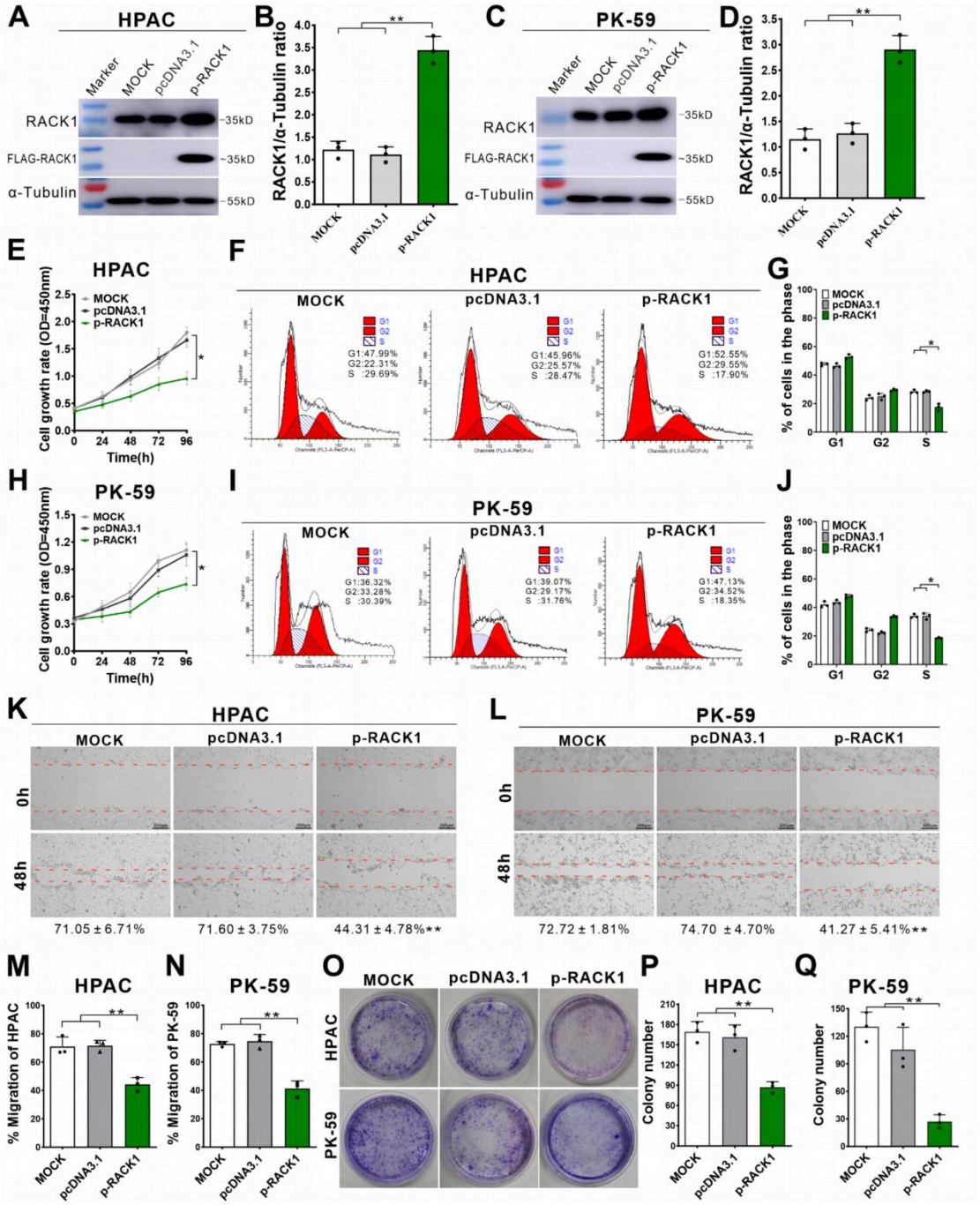

Fig. S2. Overexpression of RACK1 inhibited cell proliferation in PDA cells. (**A**-**D**) Immunoblot analysis of cell lysates from PK59 and HPAC cells transfected with MOCK, pcDNA3.1 and Flag-RACK1 plasmids. (**E**) CCK-8 assay: Overexpression of RACK1 inhibited HPAC cell growth. (**F**-**G**) Overexpression of RACK1 resulted in a decrease in the S phase transition, whereas the G1 phase population increased, with three independent experiments ($p<0.05$). (**H**) CCK-8 assay: Overexpression of RACK1 inhibited PK59 cell growth. (**I**-**J**) Overexpression of RACK1 resulted in a decrease in the S phase transition of PK59 cells, whereas the G1 phase population increased, with three independent experiments ($p<0.05$). (**K**-**N**) Scratch assay analysis: HPAC and PK59 cells transfected with MOCK, pcDNA3.1 and RACK1 plasmids ($P<0.01$). (**O**-**Q**) Colony formation assays: HPAC and PK59 cells transfected with MOCK, pcDNA3.1 and RACK1 plasmids ($P<0.01$).

Wei Zhang *et al*., Figure S3

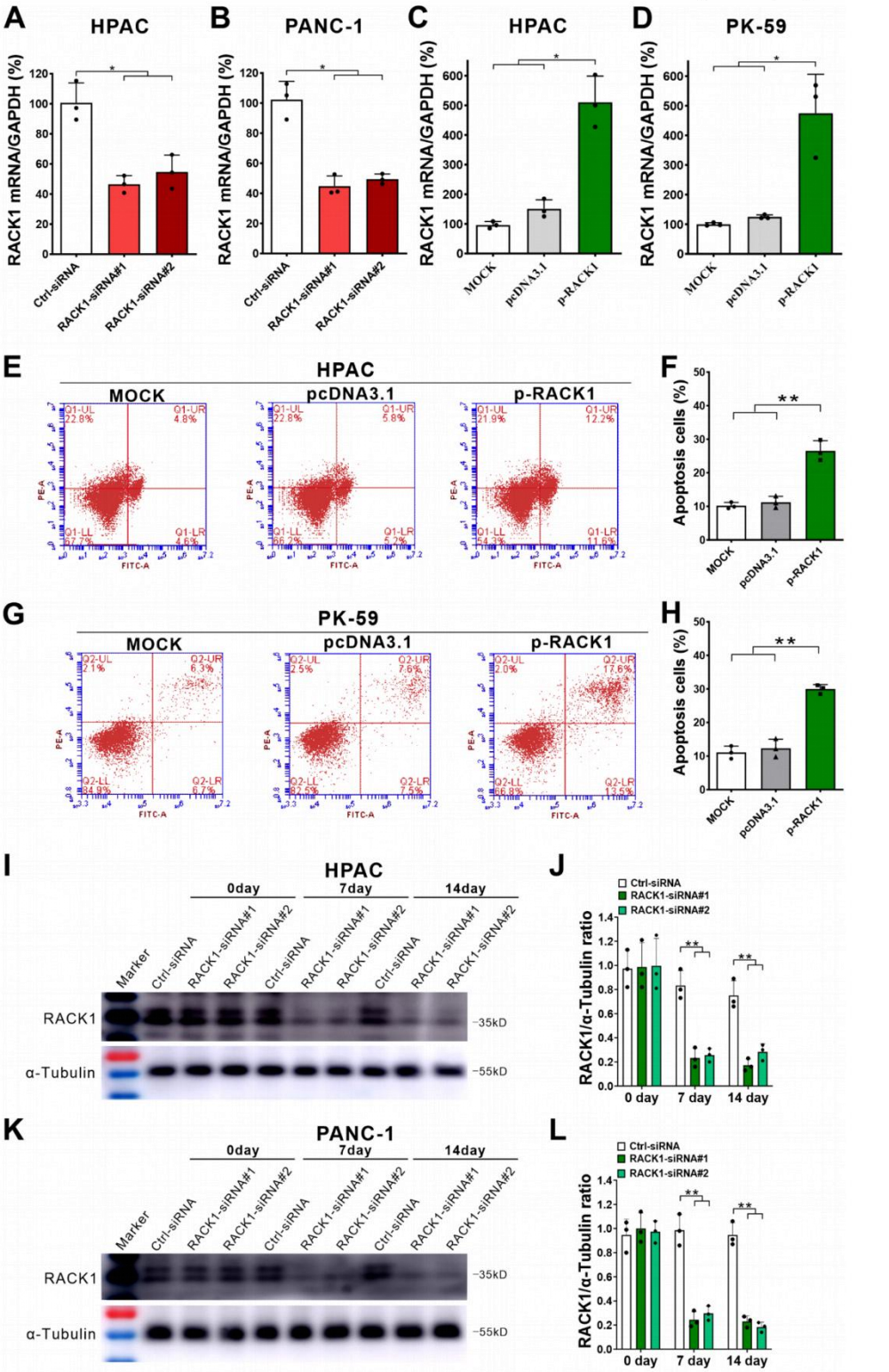

Fig. S3. Overexpression of RACK1 promoted apoptosis in PDA cells. (**A**-**B**) RT-qPCR analysis: HPAC and PANC-1 cells transfected with control siRNA, siRNA#1 and siRNA#2. (**C**-**D**) RT-qPCR analysis: PK59 and HPAC cells transfected with MOCK, pcDNA3.1, and RACK1 plasmid. (**E**-**H**) Annexin-V/PI apoptotic assay: HPAC and PK59 cells were used.

Wei Zhang *et al.*, Figure S4

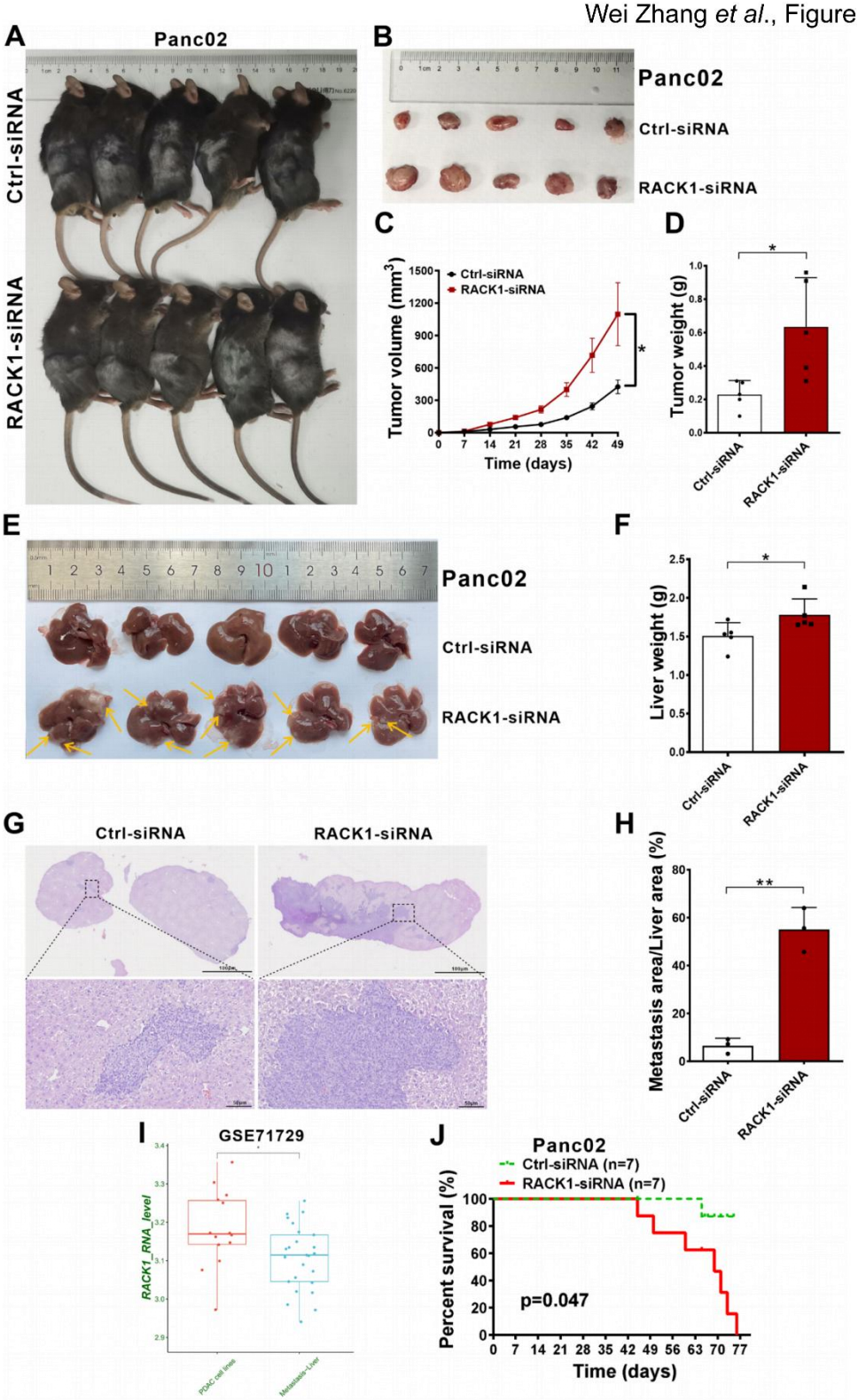

Fig. S4. RACK1 knockdown promoted pancreatic cancer growth and liver metastasis. (**A**-**B**) Representative images of Panc02 subcutaneous tumors in control siRNA, and RACK1 siRNA groups when C57BL/6 mice were sacrificed on day 45 (n=5). (**C**-**D**) Growth curves and tumor weight of Panc02 subcutaneous tumors in control siRNA, and RACK1 siRNA groups ($p<0.05$). (**E**-**F**) Representative images of liver metastasis and liver weight in control siRNA, and RACK1 siRNA groups on day 28 ($p<0.05$). (**G-H**) H&E staining and quantitative analysis of liver metastases in control siRNA, and siRNA groups. Scale bars: top row 100μm, bottom row 50μm. (**I**) RACK1 was significantly decreased in metastatic group at the mRNA level as determined by RNA-seq. (**J**) Kaplan-Meier survival curves with log-rank test were used to analyze the different effects after mice receiving intrapancreatic injection of Panc02 cells transfected with control siRNA and RACK1 siRNA ($p=0.047$).

Wei Zhang *et al.*, Figure S5

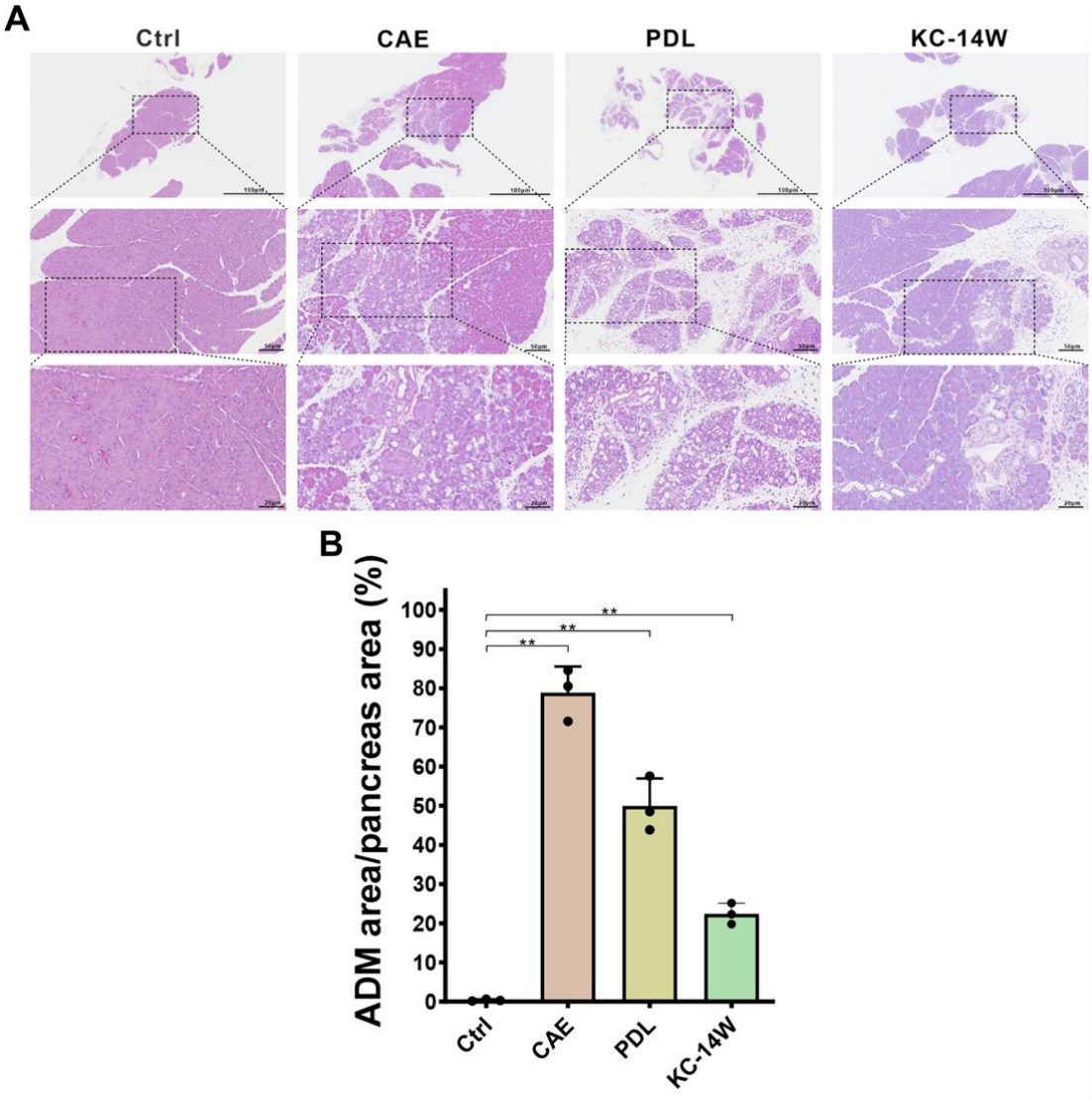

Fig. S5. H&E staining of pancreas sections. C57BL/6 control mice, CAE, PDL and KC-14W mice. C57BL/6 control mice (Ctrl: WT mice + Saline), CAE (WT mice + Caerulein), PDL (WT mice + pancreatic duct ligation) and KC-14W mice (*Pdx*-Cre; *LSL-Kras*^{G12D}).

Wei Zhang *et al.*, Figure S6

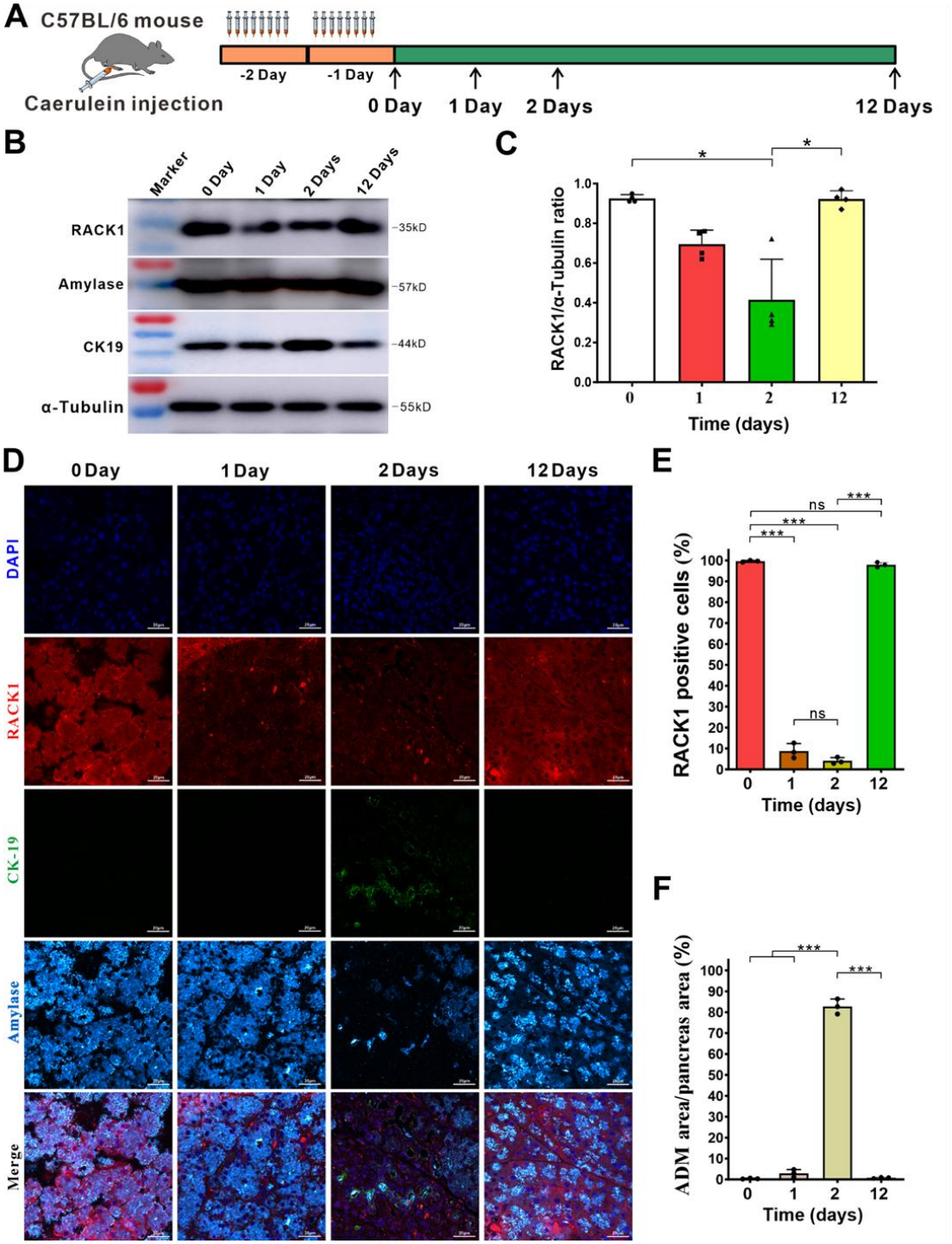

Fig. S6. The expression of RACK1 decreased during caerulein-induced acute pancreatitis and recovered during pancreas regeneration. (**A**) Scheme showing the experiment design of caerulein-induced acute pancreatitis and pancreas recovery 12 days after caerulein treatment. (**B**-**C**) Immunoblot analysis of RACK1 levels in caerulein-induced acute pancreatitis on days 0, 1, 2 and 12. (**D**) Immunofluorescence analysis of RACK1 levels in caerulein-induced acute pancreatitis on days 0, 1, 2 and 12. (**E**) Quantitative analysis of RACK1 positive cells on each day. (**F**) Quantitative analysis of ADM area/pancreas area on each day.

Wei Zhang *et al*., Figure S7

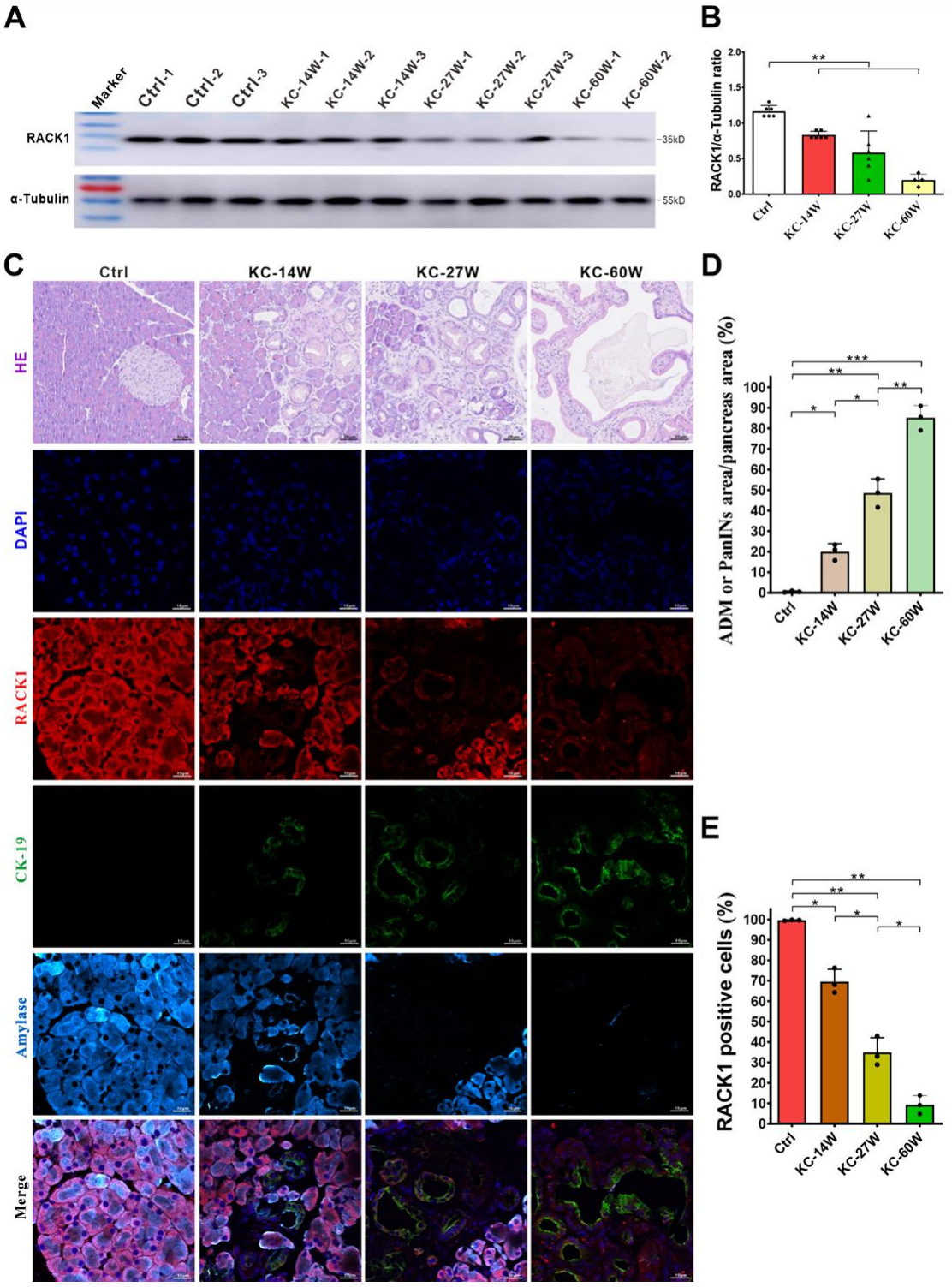

Fig. S7. The expression of RACK1 decreased in *Ptf1a*$^{+/Cre}$;*Kras*$^{+/LSL-G12D}$ mice. (**A-B**) Immunoblot analysis of RACK1 levels in C57BL/6 control mice and KC mice on 14, 27 and 60 weeks. (**C**) H&E and Immunofluorescence analysis of RACK1 levels in wild type mice and KC mice on 14, 27 and 60 weeks. (**D**) Quantitative analysis of ADM or PanINs area/pancreas area in each group. (**E**) Quantitative analysis of RACK1 positive cells in each group.

Wei Zhang *et al.*, Figure S8

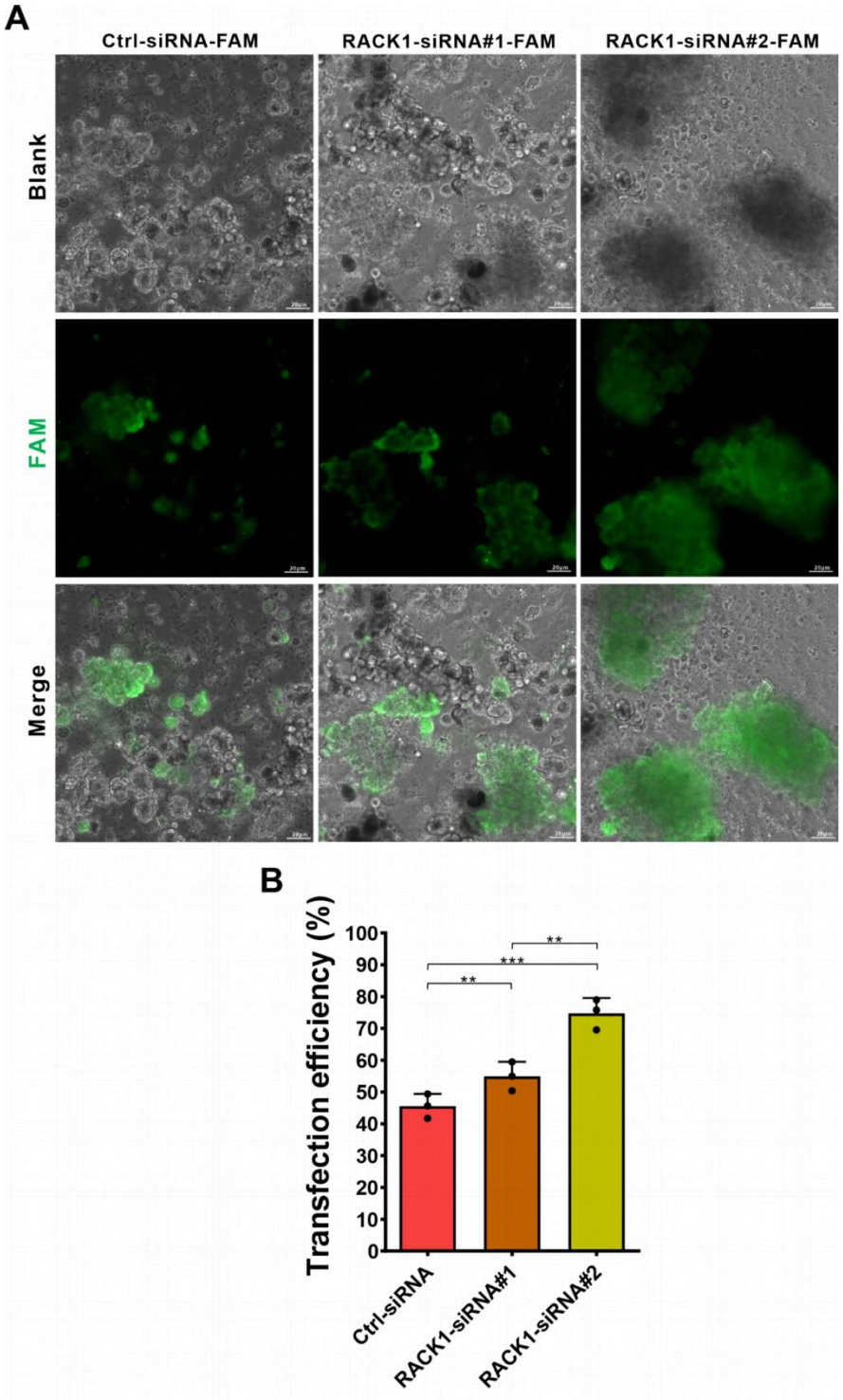

Fig. S8. Fluorescent of primary pancreatic acinar cells transfected with RACK1-siRNA-FAM. (**A**) The transfection efficiency of explant culture primary pancreatic acinar cells was confirmed by control siRNA-FAM, RACK1-siRNA#1-FAM, and RACK1-siRNA#2-FAM with green fluorescence. (**B**) The transfection efficiency of control siRNA-FAM was approximately 45%, RACK1-siRNA#1-FAM was approximately 55%, and RACK1-siRNA#2-FAM was approximately 75%.

Wei Zhang *et al.*, Figure S9

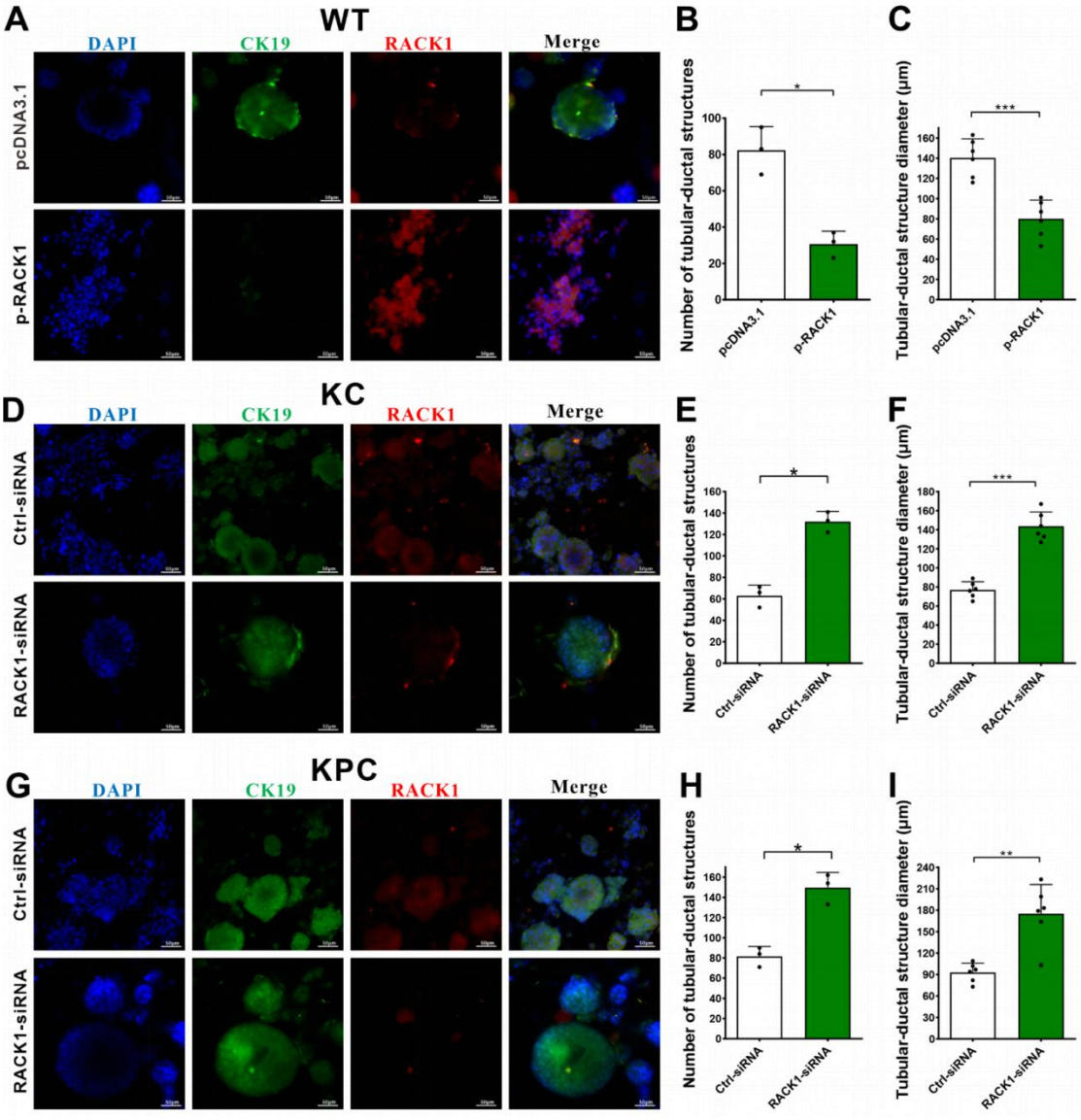

Fig. S9. Ablation of RACK1 in acinar cells accelerated ADM formation. (**A**) Immunofluorescent staining of RACK1, CK19 and DAPI in WT primary acinar cell clusters transfected with MOCK, pcDNA3.1, and RACK1 plasmid. (**B**-**C**) Quantitative analysis of tubular ductal structures and sizes in primary acinar cell explants as shown in (**A**). (**D**) Immunofluorescent staining of RACK1, CK19 and DAPI in KC primary acinar cell clusters transfected with control siRNA, RACK1 siRNA#1 and RACK1 siRNA#2. (**E**-**F**) Quantitative analysis of tubular ductal structures and sizes in primary acinar cell explants as shown in (**D**). (**G**) Immunofluorescent staining of RACK1, CK19 and DAPI in KPC primary acinar cell clusters transfected with control siRNA, RACK1 siRNA#1 and RACK1 siRNA#2. (**H**-**I**) Quantitative analysis of tubular ductal structures and sizes in primary acinar cell explants as shown in (**G**).

Wei Zhang *et al.*, Figure S10

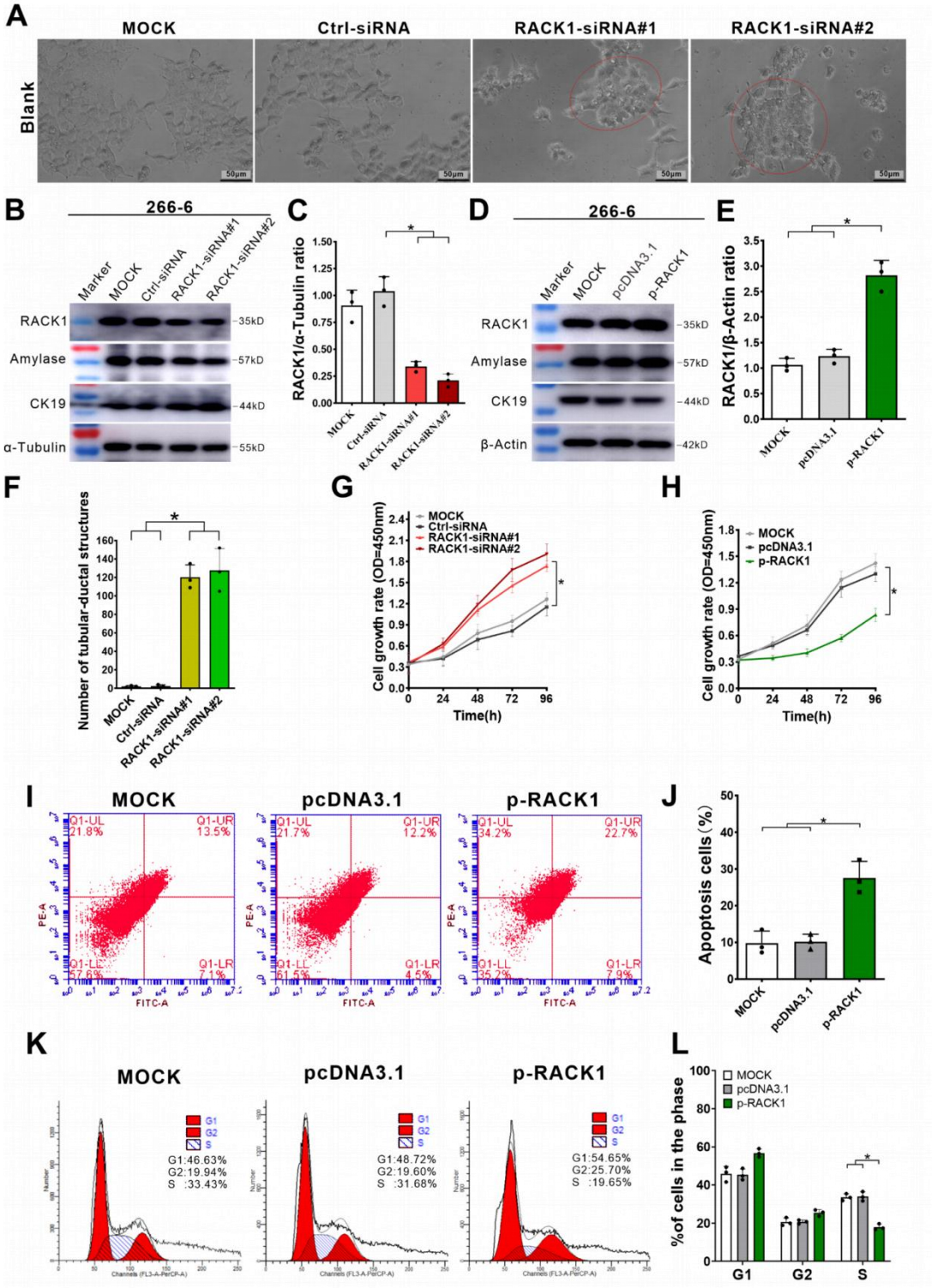

Fig. S10. Ablation of RACK1 in acinar cells accelerated ADM formation. (**A**) Brightfield images of 266-6 mouse acinar cells transfected with control siRNA, RACK1 siRNA#1 and RACK1 siRNA#2. Circle indicate ADM cells. (**B**-**C**) Immunoblot analysis of cell lysates from 266-6 acinar cells transfected with control siRNA, RACK1 siRNA#1 and RACK1 siRNA#2. (**D**-**E**) Immunoblot analysis of cell lysates from 266-6 acinar cells transfected with MOCK, pcDNA3.1 and RACK1 plasmids. (**F**) Quantitative analysis of tubular ductal structures in 266-6 acinar cells as shown in (**A**). (**G**) CCK-8 assay: Silencing RACK1 increased 266-6 acinar cell growth. (**H**) CCK-8 assay: Overexpression of RACK1 inhibited 266-6 acinar cells growth. (**I-J**) Annexin-V/PI apoptotic assay: 266-6 acinar cells. (**K-L**) Flow cytometry analysis of the cell population of 266-6 cells after transfected with RACK1 plasmid.

Wei Zhang *et al.*, Figure S11

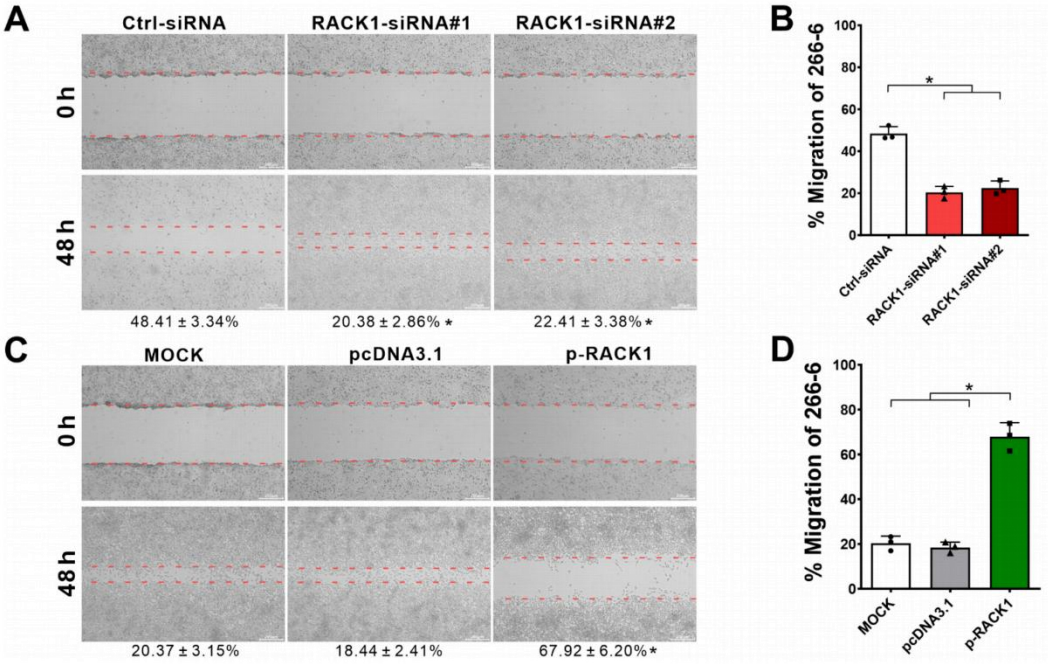

Fig. S11. Ablation of RACK1 in acinar cells accelerated cell migration. (**A**-**B**) Scratch assay analysis: cells transfected with control siRNA, RACK1 siRNA#1 and RACK1 siRNA#2 ($P<0.05$). (**C**-**D**) Scratch assay analysis: cells transfected with MOCK, pcDNA3.1 and RACK1 plasmid ($P<0.05$).

Wei Zhang *et al.*, Figure S12

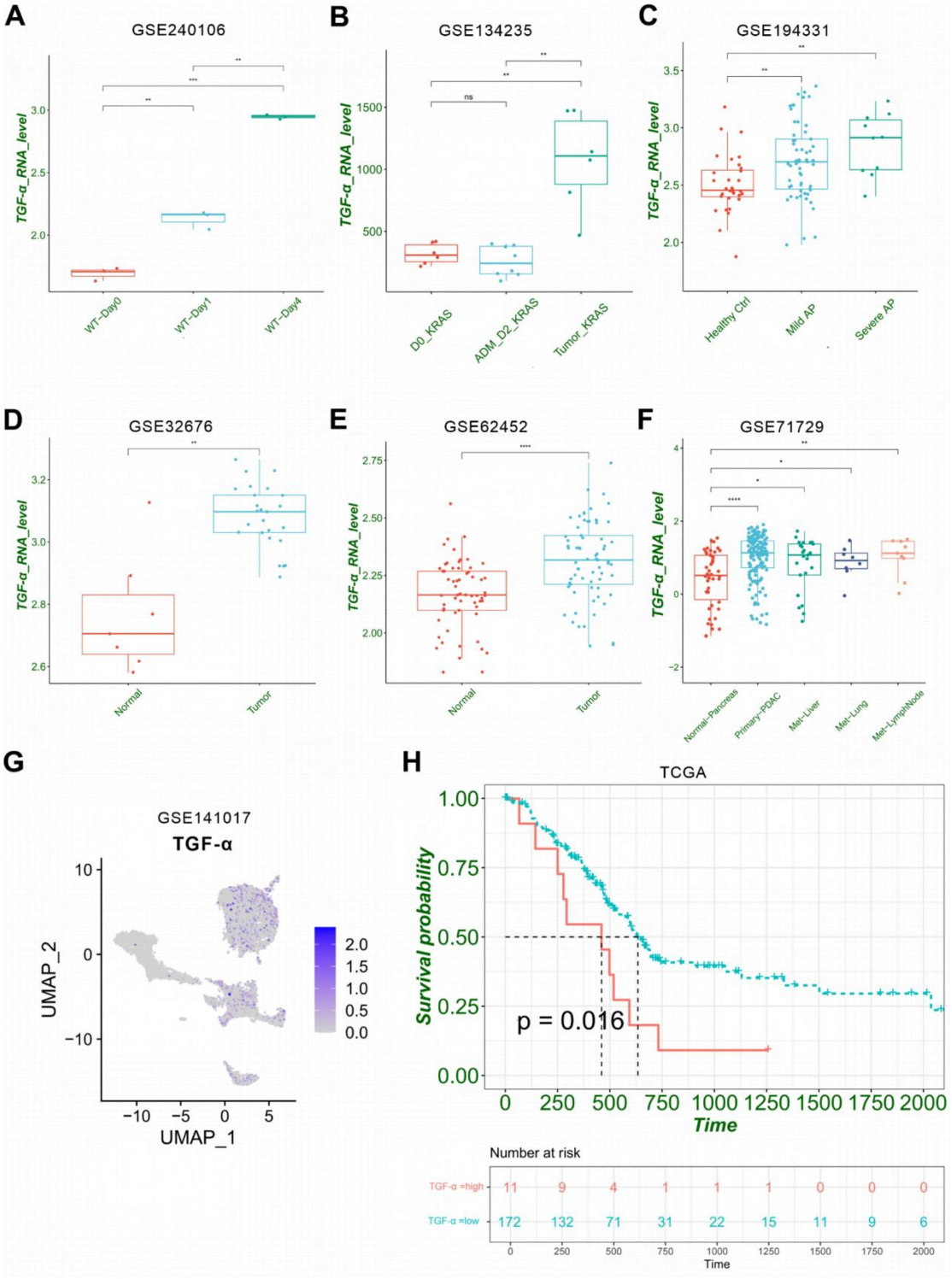

Fig. S12. TGF-α was up-regulated in PDA. (**A**) We analyzed the RNA-seq dataset (GSE240106) from normal mouse pancreatic acinar cells culture, comparing TGF-α gene expression profiles between day 1 and day 4 of culture. (**B**) We analyzed the RNA-seq dataset (GSE134235) of $KRAS^{G12D}$ mouse models. (**C**) The expression of TGF-α in acute pancreatitis. (**D-E**) The expression of TGF-α in PDA. (**F**) The expression of TGF-α in normal pancreatic tissue, primary PDAC, pancreatic cancer liver metastasis, pancreatic cancer lung metastasis, and pancreatic cancer lymph node metastasis. (**G**) The expression of TGF-α in single cell of the pancreas from PRT mice. (**H**) Kaplan–Meier survival curves of TGF-α protein expression in 183 PDA patients.

Wei Zhang *et al.*, Figure S13

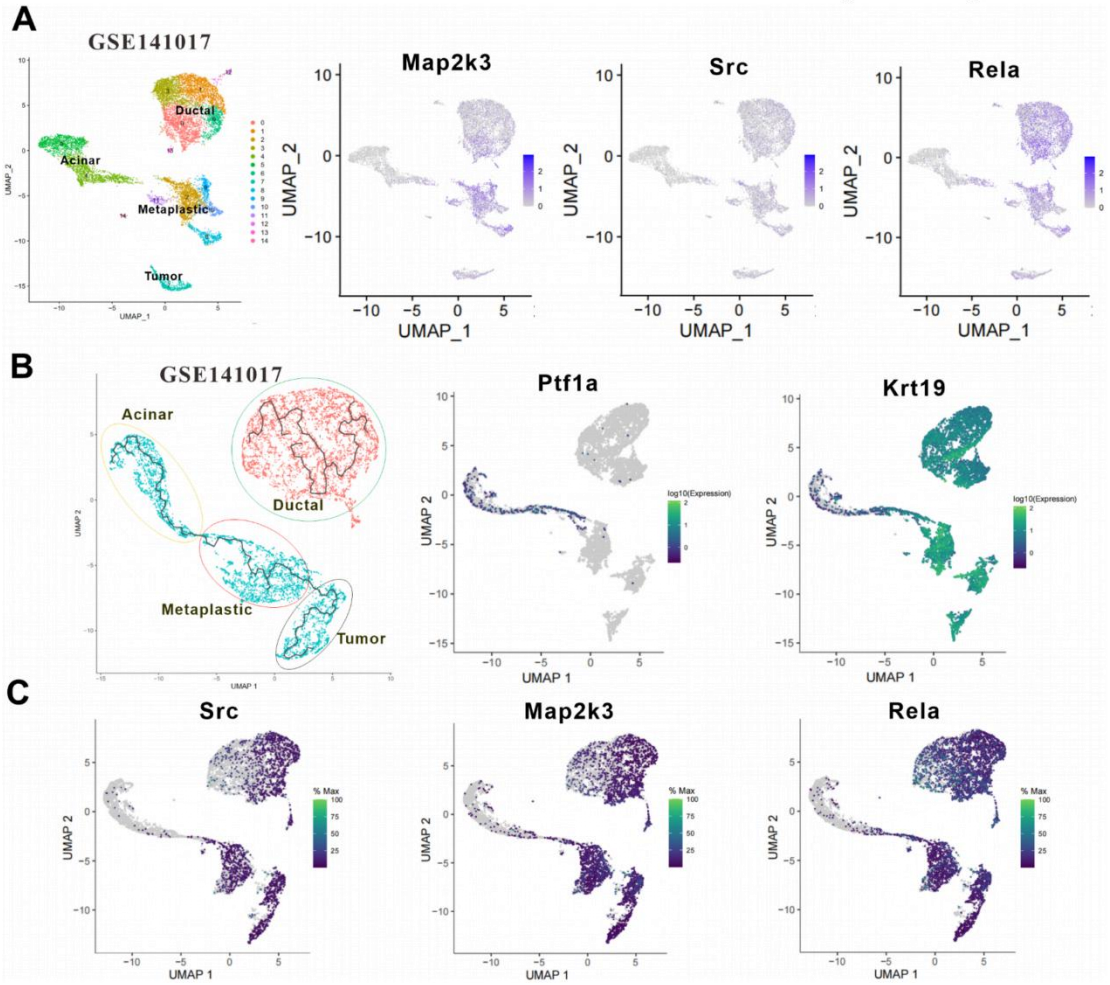

Fig. S13. Analysis of single cells of the pancreas from PRT mice. (**A**) All single cell subsets of pancreas from PRT mice. The subsets of pancreatic acinar cells, ductal cells, metaplasia cells, and tumor cells. The expression of *Map2k3*, *Src*, and *Rela* in single cell of the pancreas from PRT mice. (**B**) The trajectory predicted by Monocle3 of single cell of the pancreas in PRT mice, and the expression of acinar marker *Ptf1a*, and ductal marker *Krt19*. (**C**) The trajectory predicted of *Map2k3*, *Src*, and *Rela*.

Wei Zhang *et al.*, Figure S14

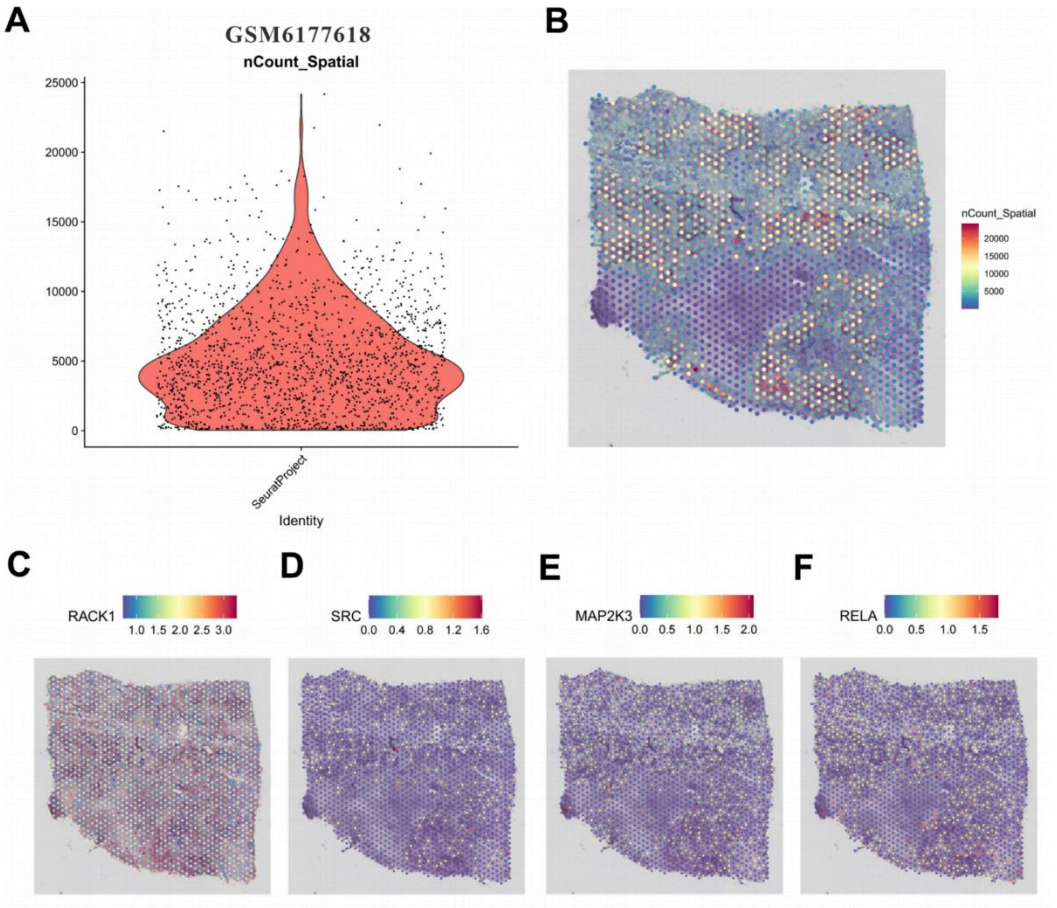

Fig. S14. The spatial transcriptomics of primary PDA. (**A**-**B**) The nCount of spatial transcriptomics of primary PDA. (**C**) The expression of RACK1 in spatial transcriptomics of primary PDA. (**D**-**F**) The expression of SRC, MAP2K3 and RELA in spatial transcriptomics of primary PDA.